Biochimica et Biophysica Acta, 765 (1984) 178–185
Elsevier

BBA 41490

ANALYSIS OF THE Chl-a_{II}^{+} REDUCTION KINETICS WITH NANOSECOND TIME RESOLUTION IN OXYGEN-EVOLVING PHOTOSYSTEM II PARTICLES FROM *SYNECHOCOCCUS* AT 680 AND 824 nm

E. SCHLODDER, K. BRETTEL, G.H. SCHATZ and H.T. WITT

Max-Volmer-Institut für Biophysikalische und Physikalische Chemie, Technische Universität Berlin, Strasse des 17. Juni 135, 1000 Berlin 12 (Germany)

(Received November 25th, 1983)

Key words: Chlorophyll a_{II} reduction; Oxygen evolution; Photosystem II; Electron transfer; (Synechococcus sp.)

The kinetics of Chl-a_{II}^{+} (P-680^{+}) reduction have been measured under repetitive excitation with nanosecond time resolution by monitoring the time-course of the absorption changes at 680 and 824 nm. O_2-evolving Photosystem II particles from *Synechococcus* sp. have been used because of the following advantages: (i) small ratio of antenna chlorophylls to Chl-a_{II} (approx. 100), (ii) low content of PS I and (iii) reduced light scattering. 1. Identical time-courses of the absorption changes at 680 and 824 nm were found in these PS II particles. 2. For the most part (approx. 70%), Chl-a_{II}^{+} is reduced in the nanosecond time range. The remaining Chl-a_{II}^{+} (approx. 30%) is reduced with half-life times in the microsecond time range. 3. The decay in the nanosecond time range is multiphasic. This multiphasic reduction can be explained quantitatively by a superposition of different reduction kinetics reported for the first single turnover flashes in dark-adapted samples (Brettel, K., Schlodder, E. and Witt, H.T. (1984) in Advances in Photosynthesis Research, Vol. 1 (Sybesma, C., ed.), pp. 295–298, Martinus Nijhoff/Dr. W. Junk Publishers, The Hague). It results a description of the nanosecond decay (approx. 70%) by three exponential phases with $t_{1/2} \approx 20$ ns (approx. 33%), ≈ 50 ns (approx. 19%) and 300 ns (approx 19%). 4. The nanosecond kinetics are attributed to electrons supplied by the oxygen-evolving complex via a secondary donor, D. For the microsecond kinetics, different suggestions are discussed. 5. The difference spectrum of the absorption changes decaying in the nanosecond time range resembles that attributed to Chl-a_{II}^{+} minus Chl-a_{II}. 6. In the absence of electron acceptors, a fast absorption change transient ($t < 6$ ns) is observed, possibly due to a charge separation and recombination between Chl-a_{II} and pheophytin. 7. Additional absorption changes observed at supersaturating flash intensities are described.

Introduction

The primary photochemical reaction in the Photosystem II reaction center is the electron transfer from the primary donor, Chl-a_{II} (P-680) [1,2], to the first stable acceptor, a special plastoquinone, PQ_1 (X-320) [3,4]. Recent studies suggest that a pheophytin molecules functions as intermediate electron carrier between Chl-a_{II} and PQ_1 [5,6]. The photooxidized Chl-a_{II} that ultimately oxidizes water is reduced by secondary donors. Thereby the oxidizing equivalents are transferred to the oxygen-evolving system by which the one-electron photooxidation of Chl-a_{II} is thought to be matched to the overall four-electron process of water oxida-

Abbreviations: Hepes, 4-(2-hydroxyethyl)-1-piperazineethanesulphonic acid; Chl, chlorophyll; Chl-a_{II}, primary electron donor of Photosystem II; D, first secondary donor of Photosystem II; DCM, 4-dicyanomethylene-2-methyl-6-*p*-dimethylaminostyryl-4H-pyran; Mes, 4-morpholineethanesulphonic acid; PMS, phenazine methosulphate; PQ, plastoquinone; PS, Photosystem.

tion leading to oxygen evolution and proton release. Studies of the re-reduction of Chl-a_{II}^{+} are carried out in order to gain insights into its functional role in photosynthetic oxygen evolution.

Flash-light induced oxidation of Chl-a_{II} was first detected by the bleaching of the red absorption band around 680 nm [1,2]. Chl-a_{II} reactions have also been measured by an absorption increase around 820 nm due to the weak infrared absorption band of the Chl-*a* cation radical [7]. A different method is based on the assumption that a change of the fluorescence yield results from the reduction of Chl-a_{II}^{+} [8–10].

Recent measurements with a sufficient time resolution of the absorption changes around 680 nm [13] and 837 nm [11] in chloroplasts under repetitive excitation show a complex multiphasic decay of Chl-a_{II}^{+}. Considering the signal-to-noise ratio and slightly different conditions, the time-course of reduction can be described consistently, at both wavelengths, by two major phases in the nanosecond range (approx. 50% with $t_{1/2} \approx 30$ ns and $\approx 20\%$ with $t_{1/2} \approx 250$ ns). The remaining 30% decay with half-life times in the microsecond range.

In the present paper we report on comparative measurements of the Chl-a_{II}^{+} reduction kinetics with nanosecond-time resolution in oxygen-evolving Photosystem II particles by following the bleaching in the red and the absorption increase in the near infrared spectral region. Thus far, the investigation of the Chl-a_{II}^{+} re-reduction in the nanosecond time range has not been performed in isolated O_2-evolving PS II particles.

The O_2-evolving PS II particles were isolated from a thermophilic cyanobacterium Synechococcus [12]. These preparations offer valuable advantages for kinetic absorption spectroscopy:

(a) a substantial improvement of the signal-to-noise ratio due to the smaller ratio of antennae pigments to the photoactive Chl-a_{II} and reduced light scattering compared to chloroplasts;

(b) practically no interference with absorption changes due to Chl-a_I (P-700) because of the low content of PS I (PS II : PS I $\gtrsim$ 20).

Therefore, these O_2-evolving PS II particles are particularly well-suited for a direct quantitative comparison between the absorption change transients at around 680 nm and 824 nm. Until now, the investigation of the Chl-a_{II}^{+} reduction kinetics has been carried out only either at around 680 or at around 820 nm.

This work has been presented in part at the Sixth International Congress of Photosynthesis, Brussels.

Materials and Methods

Cells of the thermophilic cyanobacterium Synechococcus sp. (a gift from Prof. S. Katoh, University of Tokyo) were grown at 50°C under conditions given in Ref. 12. PS II particles were prepared as described by Schatz and Witt [12] by treating isolated membranes with the zwitterionic detergent *N*-dodecyl-*N*,*N*-dimethyl-3-ammonio-1-propane sulfonate (sulfobetaine 12, SB 12). The PS II particles were finally obtained in buffer A (80% v/v), glycerol (20% v/v) and 0.3–0.4% (w/w) of the detergent SB 12. Buffer A contained $2 \cdot 10^{-2}$ M Mes/NaOH, (pH 6)/$1 \cdot 10^{-2}$ M $MgCl_2$/$2 \cdot 10^{-3}$ M KH_2PO_4/0.5 M mannitol. The chlorophyll content was determined according to Ref. 14 and was approx. 10^{-4} in the stock suspension. It was stored at -80°C for further use.

Oxygen evolution was measured with a Clark-type electrode (Rank Brothers). Under optimal conditions ($2 \cdot 10^{-2}$ M Mes/NaOH, (pH 6.5)/10^{-2} M $MgCl_2$/$2 \cdot 10^{-3}$ M KH_2PO_4/0.5 M mannitol/$2 \cdot 10^{-4}$ M phenyl-*p*-benzoquinone/$4 \cdot 10^{-6}$ M chlorophyll, and at 40°C), the rate was 0.6 O_2/Chl per s. At room temperature, the rate was 0.25 O_2/Chl per s.

The number of oxygen-evolving Photosystem II reaction centers per chlorophyll was determined by measuring the average O_2-yield in repetitive single turnover flashes under the following conditions: reaction medium containing $2 \cdot 10^{-2}$ M Mes/NaOH, (pH 6.5)/10^{-2} M $MgCl_2$/$2 \cdot 10^{-3}$ M KH_2PO_4/0.5 M mannitol/$2 \cdot 10^{-4}$ M phenyl-*p*-benzoquine; 20°C; 120 flashes averaged; flash duration, approx. 20 μs; flash repetition frequency, 2 Hz. From the result of $(2.7 \pm 0.3) \cdot 10^{-3}$ O_2/Chl per flash, we calculated a ratio Chl : Chl-$a_{II} \approx 90$.

The ratio of Photosystem II/Photosystem I reaction centers was determined by monitoring the laser flash-induced absorption change at 702 nm under the following conditions: $2 \cdot 10^{-2}$ M Hepes/NaOH (pH 7.8)/10^{-2} M $MgCl_2$/$2 \cdot 10^{-3}$ M KH_2PO_4/0.5 M mannitol/$2 \cdot 10^{-5}$ M PMS/

$2 \cdot 10^{-4}$ M sodium ascorbate/$1 \cdot 10^{-4}$ M methylviologen/$4 \cdot 10^{-6}$ M Chl. Using a value of 65000 $M^{-1} \cdot cm^{-1}$ for the differential molar extinction coefficient, we obtained PS II : PS I > 20.

The absorption changes were recorded by a repetitive flash spectrometer [15]. The sample was excited at 532 nm by a frequency-doubled Nd/YAG laser (Quantel YG 441) with a pulse-width at half-maximum amplitude of approx. 3 ns and pulse energies up to 100 mJ at a rate of 1 Hz.

The apparatus used in the 680 nm region is basically that described by Eckert [16]. The measuring light source was a dye laser (Spectra Physics 375) with $1.6 \cdot 10^{-3}$ M DCM (Exciton) as a dye in a mixture of 40% benzyl alcohol/60% ethylene glycol. It was pumped by a cw-Ar ion laser (Coherent Inova 90/5). in order to improve the stability of the measuring light intensity, the output of the dye laser passed through a noise-eater (Coherent Model 307A).

Passing through a diverging lens, the measuring laser beam was expanded (diameter of the beam at the sample, 1.5 cm). With a converging lens the virtual focus of the diverging lens was imaged through the cuvette on a diaphragm ($\varnothing = 1$ mm) placed about 1.4 m behind the cuvette. Behind the diaphragm, the measuring light beam was further focused and detected by a photodiode-preamplifier module (RCA C30847E or C30952E). By the restriction of the solid angle between the sample and the photodiode, only about $3 \cdot 10^{-8}$ of the flash-induced fluorescence was detected by the photodiode. The photodiode was further protected by a narrow-band interference filter. The remaining superimposed fluorescence has been substracted as described [13].

The signals were further amplified (HP461A or Pacific 2A50), digitized by a Biomation 6500 transient recorder and accumulated by a Nicolet 1170. The electrical bandwidth of the detection system was 1 kHz–50 MHz or 0.3 Hz–50 MHz. The signal processing system was triggered by the output of a photodiode (SGD 444, EG&G) that detected a small portion of the excitation pulse. In order to measure the wavelength of the measuring light, a portion of the beam was directed through a monochromator (Bausch and Lomb 33-86-76). The spectral resolution was approx. 1 nm. The incident measuring light intensity at the sample (approx. 120 $\mu W/cm^2$) was adjusted by increasing the intensity until a further increase changed the signal due to the excitation of the sample by the measuring light. The standard reaction medium contained; $2 \cdot 10^{-2}$ M Mes/NaOH (pH 6.5)/10^{-2} M $MgCl_2$/$2 \cdot 10^{-3}$ M KH_2PO_4/0.5 M mannitol/0.7% (v/v) glycerol/$\approx$ 0.01% (w/w) SB 12/$4 \cdot 10^{-6}$ M Chl and $2 \cdot 10^{-4}$ M phenyl-*p*-benzoquinone or $6 \cdot 10^{-4}$ M $K_3(Fe(CN)_6)$ as electron acceptor.

Absorption changes at 824 nm were measured using an apparatus described by Brettel and Witt [11] with the following modifications. The measuring light source was a laser diode (CQL12 from AEG) emitting about 8 mW at 824 nm with a spectral width of approx. 5 nm. The measuring light passed through the cuvette (optical path length: 3 cm) and was detected by a photodiode (FND 100 from EG&G) which was protected against the excitation flash and fluorescence by an interference filter. The signals were amplified (Telemeter TVV 123). Excitation of the sample and further signal processing was as described above. The electrical bandwidth was 100 Hz–100 MHz. The standard reaction mixture contained: $2 \cdot 10^{-2}$ Mes/NaOH, (pH 6.5)/10^{-2} M $MgCl_2$/$2 \cdot 10^{-3}$ M KH_2PO_4/0.5 M mannitol/4% (v/v) glycerol/$\approx$ 0.06% (w/w) SB 12/$2.5 \cdot 10^{-5}$ M Chl and $2 \cdot 10^{-4}$ M phenyl-*p*-benzoquinone or $6 \cdot 10^{-4}$ M $K_3(Fe(CN)_6)$ as electron acceptor. Deviations from this are given in the figure legends.

All measurements were performed at room temperature.

Results

Fig. 1 shows the time-course of the bleaching at 680 nm and the absorption increase around 824 nm in oxygen-evolving PS II particles. Using similar experimental conditions, the decay kinetics of the absorption change transients at 680 and 824 nm are identical in the depicted time-range within an experimental error characterized by a signal-to-noise ratio of about 20. The multiphasic decay up to 1.5 μs can be adapted by the same calculated curve (solid line in Fig. 1) assuming three exponential phases with $t_{1/2} = 20$ ns (30%), 50 ns (19%) and 280 ns (19%) (see Discussion). Fig. 2 shows that the remaining absorption change at 1.5

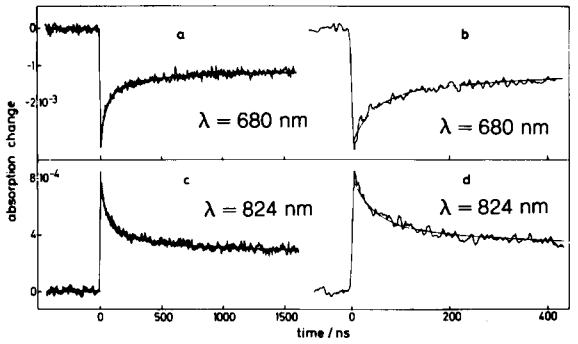

Fig. 1. Time-course of flash-induced absorption changes in the nanosecond time range attributed to Chl-a_{II} photooxidation and re-reduction at 680 (a and b) and at 824 nm (c and d) in oxygen-evolving PS II particles of the cyanobacterium Synechococcus. Excitation by 532 nm laser flashes (FWHM, approx 3 ns; repetition rate, 1 Hz). (a and b) $4 \cdot 10^{-6}$ M Chl (pH 6.5)/$2 \cdot 10^{-4}$ M phenyl-*p*-benzoquinone as e^--acceptor; excitation energy, approx. 0.4 mJ/cm^2; optical pathlength, 2 cm; electrical bandwidth; 0.3 Hz–50 MHz; average of 1280 sweeps. (c and d) $2.5 \cdot 10^{-5}$ M Chl; excitation energy, approx. 0.15 mJ/cm^2; optical pathlength, 3 cm; electrical bandwidth, 100 Hz–100 MHz; average of 580 sweeps; other conditions as in (a and b). The solid line was calculated using three exponential phases with $t_{1/2} = 20$ (30%), 50 (19%) and 280 ns (19%) plus a constant (32%).

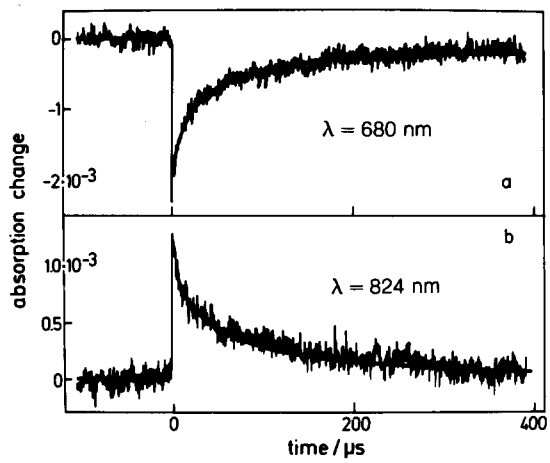

Fig. 2. Time-course of the absorption changes at 680 (a) and 824 nm (b) in the microsecond time range. Conditions as in Fig. 1, except for the following alterations; (a) $5 \cdot 10^{-6}$ M Chl/10^{-3} M $K_3(Fe(CN)_6)$ as acceptor (pH 7); excitation energy, approx. 2 mJ/cm^2; average of 256 sweeps. (b) 10^{-4} M Chl (pH 7)/10^{-3} M $K_3(Fe(CN)_6)$; excitation energy, approx. 0.7 mJ/cm^2; average of 64 sweeps. Solid lines were calculated using three exponential phases with $t_{1/2} = 5$ (12%), 38 (12%) and 200 μs (6%), assuming 30% of Chl-a_{II}^+ decay in the microsecond time range.

μs (approx. 30% of the initial amplitude, average of several measurements) decays completely up to 400–500 μs. Also, in the microsecond range, the same time-course is observed at both wavelengths. The decay in the microsecond range (approx. 30%) can be described by three phases with half-life times of 5 μs (approx. 12%), 38 μs (approx. 12%) and approx. 200 μs (approx. 6%) (solid line in Fig. 2). These microsecond half-life times are in accordance with earlier results [11,17–19].

Since the ratio of PS II : PS I is approximately equal to 20 or more in the oxygen-evolving PS II particle preparation, a contribution of Chl-a_I (P-700), the primary donor of Photosystem I, to the absorption change transients of Figs. 1 and 2 is negligible. The absence of a decay component in the millisecond range (see Fig. 2) that could be expected at 824 nm for the reduction of photooxidized Chl-a_I^+ in the presence of 1 mM ferricyanide [20] confirms this conclusion.

Fig. 3 presents the difference between the absorption change at 12 ns and 1.5 μs, i.e., essentially the amplitude of the nanosecond phases, as a function of the wavelength. The essential features are the strong bleaching at 680 nm, the development of a broad absorption band above 700 nm extending to the near infrared and the bleaching of

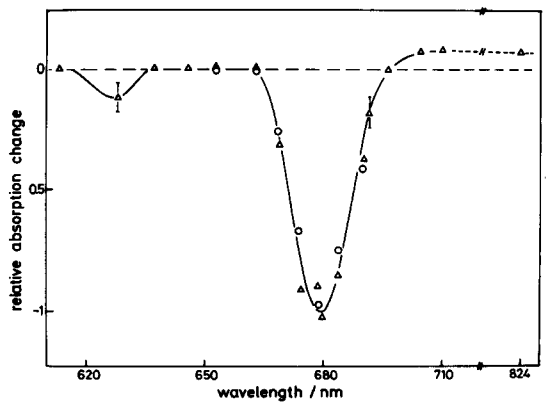

Fig. 3. Spectrum of the difference between the absorption change at 12 ns and 1.5 μs, i.e., essentially the amplitude of the nanosecond phases of the Chl-a_{II}^+ rereduction. (△) phenyl-*p*-benzoquinone and (○) $K_3(Fe(CN)_6)$ as electron acceptors.

a small band around 630 nm. The spectrum corresponds to that reported first for the 200 μs phase [2] and attributed to Chl-a_{II} [2,21,22]. Therefore, we conclude that the difference between the absorption change at 12 ns and 1.5 μs (see Fig. 3) reflects the re-reduction of photooxidized Chl-a_{II}. The extrapolated initial amplitudes under saturating conditions correspond to the following differential molar extinction coefficients per chlorophyll: $\Delta\epsilon(680\ \text{nm}) = 720 \pm 70\ \text{M}^{-1} \cdot \text{cm}^{-1}$ and $\Delta\epsilon(824\ \text{nm}) = 47 \pm 5\ \text{M}^{-1} \cdot \text{cm}^{-1}$. With a ratio of Chl : Chl-a_{II} = 90 (see Materials and Methods), we obtain $\Delta\epsilon \approx 65\,000\ \text{M}^{-1} \cdot \text{cm}^{-1}$ at 680 nm and $\Delta\epsilon \approx 4200\ \text{M}^{-1} \cdot \text{cm}^{-1}$ at 824 nm for the reaction Chl-a_{II} $PQ_1 \rightarrow$ Chl-a_{II}^+ PQ_1^-.

Through addition of NH_2OH or at low pH (pH 4), the nanosecond phases disappear and a corresponding increase of the microsecond phases (not shown) takes place. Since these treatments inhibit oxygen evolution, we can conclude that the re-reduction of Chl-a_{II}^+ in the nanosecond time-range is due to an electron transfer from the oxygen-evolving complex to Chl-a_{II}^+.

Fig. 4 compares the absorption change transients at 680 nm and 824 nm, with and without electron acceptor. Under the latter condition, the repetitive rate of the non-saturating laser flashes was changed from 1 to 5 Hz. Under these conditions the first stable acceptor, PQ_1, stays in the reduced state. This conclusion is supported by the fact that the fluorescence yield measured around 680 nm increases by a factor of 2–3 (not shown). The normal decay kinetics due to Chl-a_{II}^+ re-reduction by the secondary donors (Figs. 4a and c) were nearly absent. Instead, at both wavelengths, a very rapid transient was detected that occurs within the resolution time of the apparatus (approx. 6 ns) (Figs. 4b and d). Addition of dithionite to the sample – thus keeping PQ_1 chemically in the reduced state – had the same effect (not shown). This absorption change transient might be assigned to an electron transfer from Chl-a_{II} to an intermediate acceptor between Chl-a_{II} and PQ_1, probably a pheophytin [5,6], and the subsequent rapid recombination [6]. Based on this assumption, the absorption change is caused by the formation of the Chl-a_{II} cation and, in addition, the pheophytin anion.

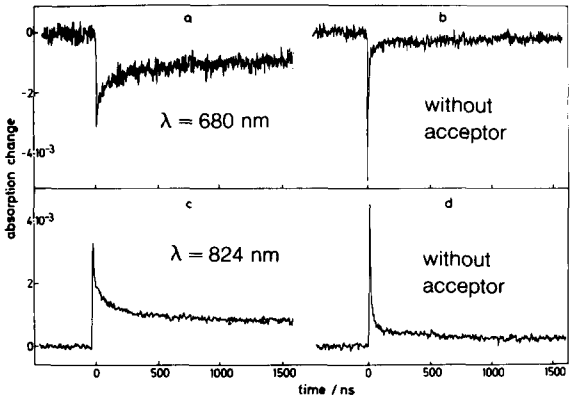

Fig. 4. Time-course of the absorption change at 680 (a and b) and 824 nm (c and d) with and without an electron acceptor. (a and c) with electron acceptor, repretition rate, 1 Hz, conditions as in Fig. 1, except for (a): excitation energy, approx. 0.4 mJ/cm^2; average of 256 sweeps, and for (c): $5 \cdot 10^{-5}$ M Chl; excitation energy, approx. 0.3 mJ/cm^2; average of 128 sweeps. (b and d) without electron acceptor, repetition rate, 5 Hz; (b) excitation energy, approx. 0.7 mJ/cm^2; average of 512 sweeps and (d) excitation energy, approx. 0.7 mJ/cm^2; average of 128 sweeps; other conditions as in (a and c).

Fig. 5 shows the saturation behaviour of the flash-induced absorption changes at 680 and 824 nm. The difference between the absorption changes at 12 ns and 1.5 μs, i.e., essentially the amplitude of the nanosecond phases, is represented by circles and the absorption change at 1.5 μs by triangles as a function of the flash energy. The flash energy was modified with neutral density filters. The solid curve has been calculated according to the following equation:

$$\text{relative absorption change} = 1 - e^{-\delta I}$$

with I = energy per cm^2 of the laser flash and δ = effective optical cross section for the Chl-a_{II} photooxidation at 532 nm. The half-saturating energies of the incident flash were approx. 0.4 mJ/cm^2 at 680 and approx. 0.37 mJ/cm^2 at 824 nm. This deviation is within the error limits caused by the accuracy of the measurement of the absolute flash energy (±10%). It should be mentioned that in Fig. 5b the amplitude of the slow phases at 824 nm (△) has been normalized, equating the amplitude at 0.37 mJ/cm^2 to 0.5, because at supersaturating energies an unknown component contributes significantly to the amplitude of the absorption change at 1.5 μs. The nature of this

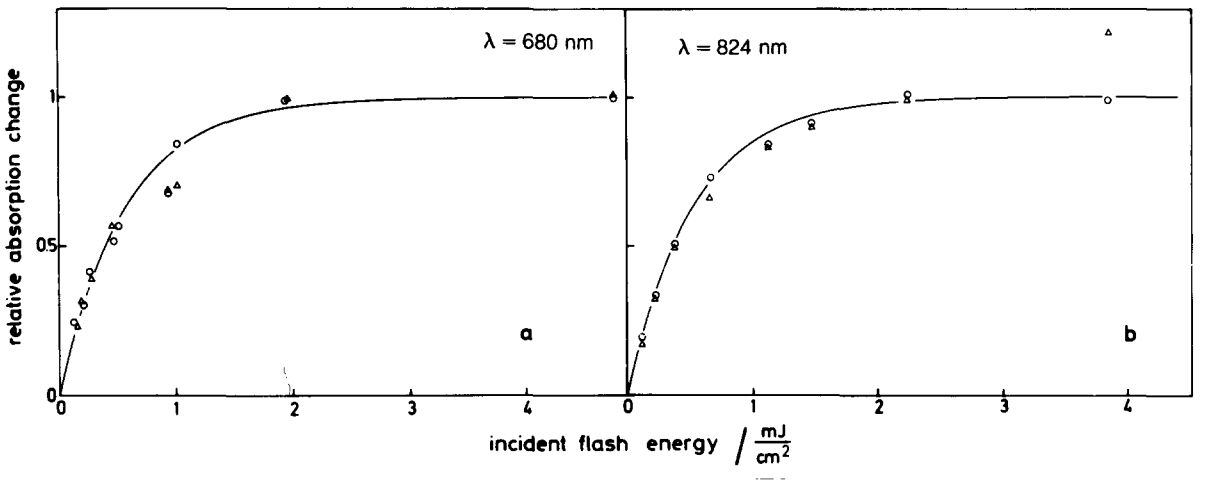

Fig. 5. Amplitude of the absorption changes as a function of the excitation flash energy at 680 (a) and at 824 nm (b). (○) amplitude of the nanosecond phases and (△) amplitude of the microsecond phases. For details see text.

superimposed signal is not yet clear. From the half saturating intensity we calculated an optical cross section of approx. $7 \cdot 10^{-16}$ cm^2 at 532 nm. This value represents a lower limit because the absorption of the excitation light within the sample was not taken into account.

In Fig. 6, the absorption changes at supersaturating excitation energies are shown. An additional, very fast absorption decrease at 680 nm and absorption increase at 824 nm becomes superimposed (compare Fig. 6 with Fig. 1). The kinetics of this transient is determined by the instrumental response time (approx. 6 ns). The amplitude does not saturate as the Chl-a_{II} reaction. Since the amplitude of this component depends in a similar way on the flash energy as the fluorescence detected at 680 nm (data not shown), we assume that this observed signal is related to a process in the antennae system and is not due to the photosynthetic electron transport. Therefore, this very fast part of the signal which can be clearly distinguished by its fast kinetics (see Fig. 6) has not been taken into account in Figs. 3 and 5 which plot the difference between the absorption change at 12 ns and 1.5 μs. It might be attributed to a Chl-triplet originating in the antennae and decaying by triplet-triplet energy transfer to the carotenoids [23]. In chloroplasts the rise time of the carotenoid triplet has been observed to be approx. 10 ns [24]. A different possibility would be the assignment to the first excited singlet state of Chl-*a* in the antennae. The observed bleaching of the red ground state absorption band and the absorption increase in the near infrared (Fig. 6) would be in accordance with the difference spectrum of Chl-*a* triplet [25,26] as well as the difference spectrum for the formation of ^{1}Chl-a* [27,28]. A fast signal (less than 6 ns) reflecting an

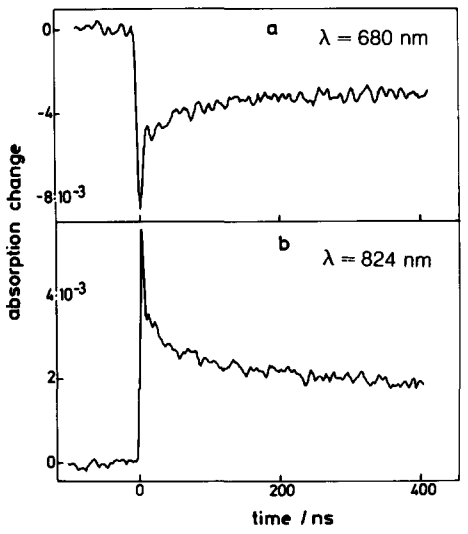

Fig. 6. Time-course of the absorption changes at 680 (a) and at 824 nm (b) at supersaturating excitation flash energies. (a) approx. 4.7 mJ/cm^2; average of 256 sweeps, (b) approx. 3.9 mJ/cm^2; average of 64 sweeps. Other conditions as in Fig. 1.

absorption decrease has also been observed at around 650 nm (not shown). It is probably caused by the accessory pigment allophycocyanin which is still attached to the PS II complex [12].

Discussion

The presented work has two aspects: (a) the investigation of the Chl-a_{II}^{+} re-reduction kinetics in oxygen-evolving PS II particles and (b) a direct quantitative comparison between the kinetics at 680 and 824 nm. Using isolated oxygen-evolving PS II particles, we could achieve, at both wavelengths, a much better signal-to-noise ratio than in previous measurements using chloroplasts [11,13]. This improvement is mainly due to the smaller ratio of antennae pigments to the photoactive Chl-a_{II} and less light scattering compared to chloroplasts. Furthermore, these preparations have the advantage that there is practically no interference with absorption changes due to Chl-a_I because of the low content of PS I (PS II : PS I $\gtrsim$ 20). Absorption changes at 700 nm due to the small Chl-a_I content have been observed only after addition of an artificial electron donor and acceptor for PS I (see Materials and Methods).

The absorption difference spectrum obtained for the Chl-a_{II}^{+} reduction in the nanosecond time-range (see Fig. 3) reflects the reaction DChl-$a_{II}^{+} \rightarrow D^{+}$Chl-$a_{II}$, where D stands for the first secondary donor. The spectrum (Fig. 3) shows predominantly features attributed to the primary donor of PS II (Chl-a_{II}^{+} minus Chl-a_{II}) [21,22]. Therefore, we assume that a contribution of the reaction $D \rightarrow D^{+}$ is negligible in the red-wavelength region. A spectrum of the difference between the absorption at 50 ns and 4 μs in chloroplasts for the region between 670 and 710 nm has been reported in Ref. 13. The slightly different spectrum, which shows the maximum of bleaching at 684 nm, might be caused by particle flattening.

The observed decay kinetics (see Figs. 1 and 2) is rather similar to that reported for chloroplasts under repetitive excitation conditions [11]. An adaptation of the decay in the nanosecond time range by two exponentials as performed in [11] is also possible with the decay shown in Fig. 1, using half-life times of approx. 22 ns (approx. 45%) and 270 ns (approx. 25%). These values match the results reported in Ref. 11 quite well. However, we prefer a description of the nanosecond decay by three exponential phases (see solid line in Fig. 1), because this adaptation is in accordance with single flash experiments [29]: different reduction kinetics of Chl-a_{II}^{+} after the first up to the fifth flash given to dark-adapted samples have been observed. Three significantly different decay times have been evaluated. A possible correlation to the different S-states of the oxygen-evolving complex has been suggested. Based on these results, we calculated the time-course of reduction under repetitive excitation where the S-states are equally populated. The result is a multiphasic decay in the nanosecond time-range characterized by three exponential phases with half-life times of approx. 20 ns (approx. 33%), approx. 50 ns (approx. 19%) and approx. 300 ns (approx. 19%). This calculated time-course agrees well with the decay of Chl-a_{II}^{+} measured under repetitive excitation (see solid line in Fig. 1). The above explanation of the multiphasic decay under repetitive excitation by a superposition of different reduction kinetics related to the different S-states is also in accordance with the observation that in dark-adapted samples after the first single turnover flash a nearly monophasic decay of Chl-a_{II}^{+} ($t_{1/2} \approx 25$ ns) was found [7,29].

The conclusion drawn from fluorescence change measurements in chlorella [8] that Chl-a_{II}^{+} is, for the most part, re-reduced in approx. 400 ns under steady-state conditions is not confirmed by our direct measurements using kinetic absorption change spectroscopy. The reason for this difference is not clear.

Since all nanosecond phases are sensitive to the inactivation of the oxygen-evolving system, we assume that these half-life times are due to the re-reduction of Chl-a_{II}^{+} by electron transfer from water via secondary donors. It had been shown earlier by Van Best and Mathis [7] that the 25 ns phase of the Chl-a_{II}^{+} decay after the first single turnover flash given to dark-adapted samples disappears through addition of NH_2OH and a corresponding increase of microsecond phases takes place. Their conclusion that the treatment with NH_2OH inactivates or modifies the normal secondary donor, D, [7] could also account for our observation.

It is not yet clear if the microsecond phases (see

Fig. 2) also reflect an electron donation from water to Chl-a_{II}^{+} (but see Refs. 18 and 30). One hesitates to decide this, because treatments inactivating the oxygen-evolving complex (addition of NH_2OH, Tris-washing, low pH, etc.) also result in decay times around 5 μs [19,31], 20–40 μs [19,31] and 100–300 μs [32,33]. Therefore, it might be suggested that the microsecond phases observed under normal conditions (approx. 30% in PS II particle preparations as well as in chloroplasts [11]) are at least in part due to a fraction which is irreversibly inactive in oxygen evolution. Another possibility would be that temporarily inactive PS II centers, corresponding to the so-called misses, contribute to the microsecond reduction kinetics. Future investigations will have to clarify to what extent PS II centers with inhibited O_2-evolution are responsible for the microsecond phases.

From the outlined measurements in oxygen-evolving PS II particles where absorption changes due to Chl-a_I do not interfere, we conclude that the Chl-a_{II} reaction can be monitored in the same manner by the bleaching at around 680 nm and by the absorption increase in the near infrared, e.g., at 824 nm.

The conclusion is based on the following evidence: (1) the identical decay kinetics over the whole time-range (see Figs. 1 and 2); (2) the similar sensitivity to treatments as for example the inactivation of the oxygen-evolving complex or the reduction of the first stable electron acceptor, PQ_1 (see Fig. 4), and (3) the same light saturating behaviour (see Fig. 5).

Acknowledgements

The authors thank Ms. Irene Geisenheimer for preparing the PS II particles and Dr. H.-E. Buchwald for valuable technical help with the experimental apparatus. This work was supported by grants from the Deutsche Forschungsgemeinschaft (Sonderforschungsbereich 9, Teilprojekt C9).

References

1 Döring, G., Stiehl, H.H. and Witt, H.T. (1967) Z. Naturforsch. 22b, 639–644
2 Döring, G., Renger, G., Vater, J. and Witt, H.T. (1969) Z. Naturforsch. 24b, 1139–1143
3 Stiehl, H.H. and Witt, H.T. (1968) Z. Naturforsch. 23b, 220–224
4 Stiehl, H.H. and Witt, H.T. (1969) Z. Naturforsch, 24b, 1588–1598
5 Klimov, V.V., Klevanik, A.V., Shuvalov, V.A. and Krasnovsky, A.A. (1977) FEBS Lett. 82, 183–186
6 Shuvalov, V.A., Klimov, V.V., Dolan, E., Parson, W.W. and Ke, B. (1980) FEBS Lett. 118, 279–282
7 Van Best, J.A. and Mathis, P. (1978) Biochim. Biophys. Acta 505, 178–188
8 Mauzerall, D. (1972) Proc. Natl. Acad. U.S.A. 69, 1358–1362
9 Sonneveld, A., Rademaker, H. and Duysens, L.N.M. (1979) Biochim. Biophys. Acta 548, 536–551
10 Deprez, J., Dobek, A., Geacintov, N.E., Paillotin, G. and Breton, J. (1983) Biochim. Biophys. Acta 725, 444–454
11 Brettel, K. and Witt, H.T. (1983) Photobiochem. Photobiophys. 6, 253–260
12 Schatz, G.H. and Witt, H.T. (1984) Photobiochem. Photobiophys. 7, 1–14
13 Eckert, H.-J., Renger, G. and Witt, H.T. (1984) FEBS Lett. 167, 316–320
14 McKinney, G. (1941) J. Biol. Chem. 140, 315
15 Rüppel, H. and Witt, H.T. (1969) Meth. Enzymol. 16, 316–380
16 Eckert, H.J. (1982) Thesis, Technische Universität Berlin
17 Gläser, M., Wolff, Ch., Buchwald, H.E. and Witt, H.T. (1974) FEBS Lett. 42, 81–85
18 Renger, G., Eckert, H.J. and Buchwald, H.E. (1978) FEBS Lett. 90, 10–14
19 Conjeaud, H., Mathis, P. and Paillotin, G. (1979) Biochim. Biophys. Acta 546, 280–291
20 Rumberg, B. and Witt, H.T. (1964) Z. Naturforsch. 19b, 693–707
21 Van Gorkom, H.J., Tamminga, J.J., Haveman, J. and Van der Linden, I.K. (1974) Biochim. Biophys. Acta 347, 417–438
22 Ke, B., Inoue, H., Babcock, G.T., Fang, Z. and Dolan, E. (1982) Biochim. Biophys. Acta 682, 297–306
23 Wolff, C. and Witt, H.T. (1969) Z. Naturforsch. 24b, 1031–1037
24 Kramer, R. and Mathis, P. (1980) Biochim. Biophys. Acta 593, 319–329
25 Seifert, K. and Witt, H.T. (1968) Naturwiss. 55, 222
26 Mathis, P. and Setif, P. (1981) Isr. J. Chem. 21, 316–320
27 Shepanski, J.F. and Anderson, R.W. (1981) Chem. Phys. Lett. 78, 165–173
28 Huppert, D., Rentzepis, P.M. and Tollin, G. (1976) Biochim. Biophys. Acta 440, 356–364
29 Brettel, K., Schlodder, E. and Witt, H.T. (1984) in Advances in Photosynthesis Research, Vol. 1 (Sybesma, C., ed.), pp. 295–298, Martinus Nijhoff/Dr. W. Junk Publishers, The Hague
30 Gläser, M., Wolff, Ch. and Renger, G. (1976) Z. Naturforsch. 31c, 712–721
31 Conjeaud, H. and Mathis, P. (1980) Biochim. Biophys. Acta 590, 353–359
32 Haveman, J. and Mathis, P. (1976) Biochim. Biophys. Acta 440, 346–355
33 Renger, G. and Wolff, Ch. (1976) Biochim. Biophys. Acta 423, 610–614